



Contents lists available at ScienceDirect

Arabian Journal of Chemistry

journal homepage: www.ksu.edu.sa

Original article

Optimizing coolant oil wastewater treatment via modified air-Fenton process with bimetallic particles from auto parts manufacturing waste

 Hathaichanok Suannuch^{a,b}, Vorapot Kanokkantapong^{c,d,*}, Jatuwat Sangsanont^{c,e}
^a International Postgraduate Programme in Hazardous Substance and Environmental Management, Graduate School, Chulalongkorn University, Bangkok 10330, Thailand

^b Center of Excellence on Hazardous Substance Management (HSM), Chulalongkorn University, Bangkok 10330, Thailand

^c Department of Environmental Science, Faculty of Science, Chulalongkorn University, Bangkok 10330, Thailand

^d Waste Utilisation and Ecological Risk Assessment Research Unit, Chulalongkorn University, Bangkok 10330, Thailand

^e Water Science and Technology for Sustainable Environmental Research Unit, Chulalongkorn University, Bangkok 10330, Thailand


ARTICLE INFO

Keywords:

 Wastewater treatment
 Cutting oil
 Waste utilisation
 High COD wastewater
 Advanced oxidation processes
 Modified air Fenton (MAF)
 Bimetallic particles

ABSTRACT

This study evaluated the efficiency of aluminium (Al)/iron (Fe) bimetallic particles, produced from waste by-products of auto parts manufacturing—namely, aluminum dross (AD) and shot blast (SB)—in removing chemical oxygen demand (COD) and total organic carbon (TOC) from coolant oil wastewater originating from an auto parts manufacturer. Two different molar ratios of ADSB bimetallic particles, namely, 1:1 (ADSB1) and 2:1 (ADSB2), were investigated for their characteristics and applied in the modified air-Fenton (MAF) process which enhances the traditional Fenton method by utilizing ADSB bimetallic particles instead of Fe⁰ and Al⁰, and by incorporating aeration to stimulate the reaction. The wastewater contained an initial COD ranging from 60,000 to 120,000 mg L⁻¹ (at 3–5 % v/v) and a TOC ranging from 10,000 to 40,000 mg L⁻¹. The experimental design included varying reaction times, pH values, quantities of bimetallic particles, airflow rates, and wastewater concentrations were performed using the Minitab-19 software package. X-ray fluorescence (XRF) analysis revealed that the bimetallic particles have SiO₂ content ranging from 39.69 % to 56.03 %, Fe₂O₃ ranging from 20.52 % to 30.90 % and Al₂O₃ ranging from 16.51 % to 16.66 %, with surface areas varying between 5 and 6 m² g⁻¹. As a result of XRF analysis, SiO₂ can be contaminated by the sand molds used in the manufacturing process of products. Notably, ADSB1 exhibited impressive removal efficiencies of 98.70 % and 98.50 % for COD and TOC, respectively, at 0.6 g, pH 3, airflow rate of 1.5 L min⁻¹, and reaction time of 105 min. Conversely, ADSB2 achieved removal efficiencies of 96.30 % and 98.43 % for COD and TOC, respectively, at 0.2 g, pH 9, airflow rate of 2.0 L min⁻¹, and reaction time of 180 min. Pareto charts and 3D surface plots derived from the data showed the number of bimetallic particles as the most influential factor, followed by the initial pH. The MAF process significantly extends the pH range under diverse conditions by incorporating ADSB particles and reduces the reliance on traditional chemicals like hydrogen peroxide. This research presents a promising advancement in wastewater treatment technology.

1. Introduction

The automobile component manufacturing sector in Thailand is a significant and prosperous industry. A notable portion of this waste consists of aluminium dross (AD) and shot blast (SB) residues, byproducts of automobile manufacturing processes, which contain substantial amounts of aluminium and iron. Recycling and reusing these wastes, especially in the form of bimetallic particles, could offer a promising solution for waste reduction and recycling, while unlocking new sources

of valuable metals (Mahinroosta and Allahverdi, 2018; Lermen et al., 2020).

The global water shortage and the continuous depletion of water resources, coupled with the growth of human communities and the production of various chemicals in industries, underscore the urgent need for efficient water and wastewater treatment methods (Rostami et al., 2021). Wastewater from automobile component manufacturing, characterized by high levels of refractory organic pollutants and elevated concentrations of chemical oxygen demand (COD) and total

* Corresponding author at: Department of Environmental Science, Faculty of Science, Chulalongkorn University, Bangkok 10330, Thailand.

E-mail address: Vorapot.ka@chula.ac.th (V. Kanokkantapong).

<https://doi.org/10.1016/j.arabjc.2024.105860>

Received 15 March 2024; Accepted 1 June 2024

Available online 13 June 2024

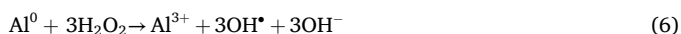
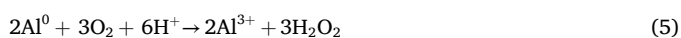
1878-5352/© 2024 The Author(s). Published by Elsevier B.V. on behalf of King Saud University. This is an open access article under the CC BY-NC-ND license (<http://creativecommons.org/licenses/by-nc-nd/4.0/>).

organic carbon (TOC), requires direct chemical treatment to prevent environmental and public health risks (Amin et al., 2017).

Advanced oxidation processes (AOPs) have become essential for treating industrial wastewaters due to their ability to generate highly potent and non-selective oxidizing agents, such as hydroxyl radicals, which effectively degrade refractory and hazardous pollutants (Shokri, 2016). Among AOPs, semiconductor photocatalysts are notable for achieving the complete mineralization of pollutants (Shokri and Mahanpoor, 2018). The advanced Fenton process is emerging as a promising solution for treating wastewater, offering a more efficient and economical alternative to the conventional Fenton process. Nano and micro-scale zero-valent iron (ZVI) and various iron-supported activators are utilized in the advanced Fenton process to generate radicals through the modified air-Fenton (MAF) process, improving productivity and reducing costs (Yildiz et al., 2022; Srimoke et al., 2022).

Particularly intriguing is the generation of hydroxyl radicals when zero-valent iron (Fe^0) (ZVI) or other metals interact with oxygen in an aqueous environment, resulting in the formation of various radical species (Chen et al., 2008; Phinjaroenphan et al., 2021). Further investigations are warranted to optimize the efficacy of metal ions in this reaction.

In addition, the combination of two different metals, known as 'bimetallic particles', exhibits not only the individual characteristics of its constituents but also novel and improved properties arising from the synergistic effect of the metals. These bimetallic particles can serve as catalysts in oxidation processes for eliminating contaminants present in wastewater, which are frequently used in the Fenton process (Phinjaroenphan et al., 2021). The use of bimetallic particles in the MAF process leads to enhanced operational efficiency and reduced costs, with the noteworthy aspect of using industrial wastes in their production. The MAF process reactions are described by the following equations (Chen et al., 2008, Babuponnusami and Muthukumar, 2014, Saber et al., 2014, Xiong et al., 2015, Wang and Tang, 2021, Rapeephun et al., 2022):



To address the treatment of various pollutants present in coolant oil wastewater, the MAF procedure using bimetallic particles was explored. Bimetallic particles prepared from AD and SB, considering variables such as reaction time, pH, quantity of bimetallic particles, airflow rate, bimetallic particle ratio and wastewater concentration were conducted. Furthermore, the surface area, metal composition of bimetallic particles and proposed mechanism for the generation of bimetallic particles and OH^\bullet in the MAF process applied for coolant oil treatment were examined. This study introduces a compelling environmental management approach known as 'trash-to-treasure.' This method involves repurposing waste from one manufacturing facility to treat wastewater from another factory, all within the same manufacturing process.

2. Materials and methods

2.1. Chemicals in the MAF study

All the chemicals utilised in this study were of analytical reagent

grade, requiring no further purification, except for the recycled AD and SB wastes obtained from auto parts production. The synthetic coolant oil wastewater was prepared using soluble coolant oil commercially available in Winnex Co., Thailand. Isopropanol was used as a radical scavenger during the MAF process to determine the types of free radicals generated.

2.2. Bimetallic particles

2.2.1. Auto parts manufacturing waste collection and bimetallic particle preparation

Initially, AD and SB scraps were subjected to pulverisation using a ball mill at speeds ranging from 5000 to 13,000 rounds per hour. This process yielded a powder with particle sizes ranging from 210 μm (sieve No. 70) to 500 μm (sieve No. 35). To investigate the impact of varying aluminium contents on the MAF process for treating coolant oil wastewater, bimetallic particles were prepared in two distinct molar ratios, namely, 1:1 (ADSB1) and 2:1 (ADSB2) aluminium to iron ratios.

2.2.2. Bimetallic particle synthesis

To synthesize ADSB1 bimetallic particles, 7.5 g of SB and 55.55 g of AD were mixed with 30 mL of deionized water to improve the solubility of the AD powder. Subsequently, 30 mL of HCl solution was added to remove any oil contaminants remaining on the surface of the waste. The solution was thoroughly mixed and filtered through a No. 2 filter paper (Whatman™, England) to separate the liquid phase from the solid phase, which contained the bimetallic particles. The particles were then dried at 80 °C for 2 h and subsequently ground using a mortar and pestle to obtain the ADSB1 powder with uniform grain size. ADSB2 particles were prepared in a similar manner, but with double the AD content. Both samples of bimetallic particles were stored in a desiccator at room temperature to preserve their characteristics for future use.

2.3. Bimetallic and wastewater characteristic analysis

The surface morphology, elemental compositions and physical properties of the ADSB1 and ADSB2 samples were examined via scanning electron microscopy (SEM; JSM-6610 LV, JEOL, Tokyo, Japan) and energy-dispersive X-ray spectroscopy (EDS; INCAx-act, Oxford Instruments, Oxford, UK), respectively. In addition, their crystalline phases were identified and quantified through X-ray diffraction (XRD) patterns (D8 DISCOVER, Bruker, Massachusetts, US) and X-ray fluorescence (XRF) spectra (S4 PIONEER, Bruker, Massachusetts, US). Surface area analysis was conducted using the Brunauer–Emmett–Teller (BET) method, which involved N_2 adsorption (TriStar II Plus 3.02, Micromeritics, Norcross, GA, USA). The quantification of COD followed the closed flux standard procedures method 5220C, whereas TOC analysis was conducted using a TOC analyser (NC-3100, Analytic Jena Far East (Thailand) Ltd.).

2.4. Coolant oil wastewater synthesis

A synthetic coolant oil wastewater was prepared using a commercial coolant fluid to replicate the characteristics of wastewater discharged during auto parts manufacturing. A commercial cutting fluid was diluted to a concentration of 3–5 % v/v to simulate a COD range of approximately 60,000–120,000 mg L^{-1} , similar to real industrial wastewater. A 3 % v/v mixture was prepared by combining 30 mL of cooling oil with 1000 mL of deionised water in a volumetric flask. To achieve 4 % or 5 % v/v ratios, the volume of the cooling oil was adjusted to 1000 mL while maintaining the appropriate proportions. The synthetic coolant oil wastewater was then stored in a glass container placed in a cabinet.

Table 1
Coded and actual values of the DOE variables for the MAF process.

Variable	Unit(s)	Factor levels		
		-1	0	+1
Bimetallic quantity	g	0.20	0.60	1.00
Initial pH	-	3	4	5
Reaction time	min	30	105	180
Airflow rate	L min ⁻¹	1.0	1.5	2.0
Wastewater concentration	% v/v	3	4	5

Table 2
CCD design by the Minitab-19 programme for the MAF process with bimetallic particles.

Bimetallic (g)	pH	Time (min)	Airflow rate (L min ⁻¹)	Wastewater concentration (mg L ⁻¹)
0.2	3	180	2.0	120,000
0.2	3	30	1.0	120,000
0.6	6	105	1.5	80,000
1.0	9	180	2.0	120,000
0.6	3	105	1.5	80,000
1.0	9	30	1.0	120,000
1.0	6	105	1.5	80,000
0.2	9	30	1.0	60,000
0.2	9	30	2.0	120,000
0.6	6	180	1.5	80,000
1.0	3	180	1.0	120,000
0.6	6	105	1.0	80,000
0.6	6	30	1.5	80,000
1.0	3	30	1.0	60,000
0.2	3	180	1.0	60,000
0.6	6	105	1.5	80,000
1.0	9	105	1.5	80,000
0.2	3	30	2.0	60,000
1.0	3	180	2.0	60,000
0.2	9	180	2.0	60,000
0.6	6	105	1.5	80,000
0.6	6	105	2.0	80,000
0.6	6	105	1.5	60,000
0.6	6	105	1.5	80,000
0.2	9	180	1.0	120,000
1.0	3	30	2.0	120,000
0.6	6	105	1.5	120,000
1.0	9	30	2.0	60,000
0.2	6	105	1.5	80,000

2.5. Experimental design of synthetic coolant oil wastewater treatment via the MAF process using bimetallic particles

Throughout the experiment, the Minitab-19 statistical software (<http://www.minitab.com/en-us/products/minitab>) was used to thoroughly investigate all the design parameters. The MAF process, in which bimetallic particles were used, was employed to treat synthetic coolant oil wastewater at room temperature. A batch experiment was conducted to determine the optimal conditions for synthetic coolant oil wastewater treatment using the central composite design (CCD) analysis in Minitab-19 to identify the most suitable operating conditions.

2.5.1. Design of the experiment for optimization

The design of experiments (DOE) approach was employed to determine the optimal parameters for treating synthetic coolant oil wastewater using the MAF process with bimetallic particles. This approach incorporated the response surface methodology-associated designs methodology in the CCD analysis. The CCD analysis involves central and axial points, along with cube points, after the elimination of insignificant factors using screening techniques. It enables the creation of a response surface regression curve and facilitates the calculation of higher-order effects.

The study parameters included bimetallic quantity (A), initial pH (B),

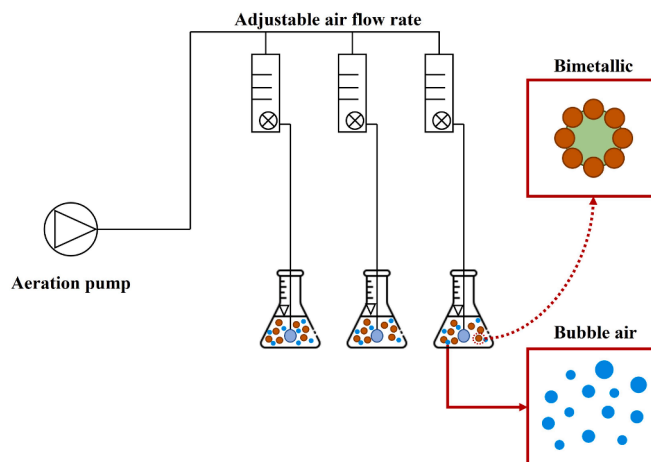


Fig. 1. Schematic diagram of the laboratory experimental setup for the MAF process.

reaction time (C), airflow rate (D) and wastewater concentration (E). The coded and actual values of these variables are listed in Table 1. The actual values represented the initially assigned values for each factor, whereas the coded values were provided for the different levels of factors by default or were adjustable. In this context, variables A, B, C, D and E were considered to be actual and coded factors.

The total number of experimental runs was increased threefold, which resulted in 90 runs for each bimetallic particle sample. Minitab-19 was used to assess the removal efficiency of COD and TOC. Both the ADSB1 and ADSB2 bimetallic particles were subjected to the MAF process to evaluate the removal efficiency of COD and TOC as dependent variables, considering the aluminium and iron contents. The study explored five independent variables, including the quantity of bimetallic particles (0.20–1.00 g), reaction time (30–180 min), airflow rate (1.0–2.0 L min⁻¹), initial wastewater pH (3–9) and wastewater concentration (3–5 % v/v). The parameters of all experiments conducted in this study are listed in Table 2.

2.5.2. MAF process experiments

The MAF process was started by 50 mL of synthetic coolant oil wastewater with ADSB bimetallic particles. The aeration pump was activated to infuse air into the wastewater for specific reaction times, as shown in Table 2. After completion, the reaction was terminated by adjusting the pH to 8 using NaOH. Subsequently, the bimetallic particles settled for 2 h at the base of the cylindrical beaker. The treated wastewater was collected and preserved by adjusting its pH to 2 using H₂SO₄. The efficiency of wastewater removal was calculated as follows:

$$\text{Removal efficiency} = \frac{C_0 - C_t}{C_0} \times 100 \quad (8)$$

where C_0 denotes the initial value of COD and TOC and C_t denotes the value at time t . A schematic representation of the laboratory experimental setup utilised for the MAF process is shown in Fig. 1.

2.6. Effect of a scavenger determinations

The experiment aimed to study the scavenger effect in the MAF process, targeting a 95 % removal efficiency as the benchmark. The MAF batch experiment was meticulously designed according to the outlined parameters. For the scavenger analysis, isopropyl alcohol (IPA) was selected due to its rapid reactivity with OH[•] radicals in the Fenton reaction. IPA was introduced into the reactor to quickly react with the radicals in the wastewater during the MAF operation.

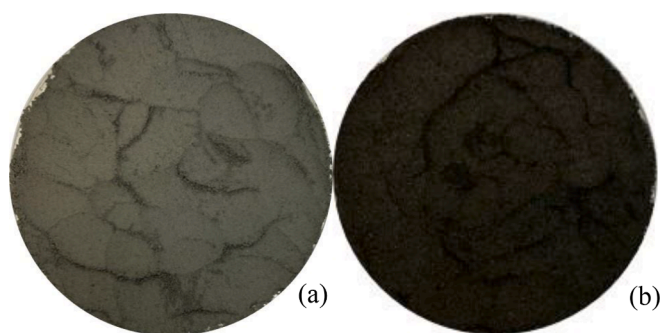


Fig. 2. Auto parts manufacturing waste: (a) AD and (b) SB.

3. Results and discussion

3.1. Auto parts manufacturing waste and bimetallic particle characterisation

3.1.1. Auto parts manufacturing waste characterisation

Fig. 2 illustrates the morphological characteristics of AD and SB before their application in the synthesis of bimetallic particles. AD is shown in Fig. 2a, displaying a grey hue, likely stemming from the utilisation of aluminium constituents in auto parts manufacturing.

Conversely, SB is shown in Fig. 2b, exhibiting a black colour attributed to its iron composition.

The geometries and surface areas of AD and SB were assessed via SEM-EDS analysis, as depicted in Fig. 3. In the case of AD, two distinctive colour phases were discernible, indicative of varying sand components potentially present in the AD waste (Fig. 3a). The structure of SB waste is presented in a rectangular configuration in Fig. 3b. Notably, the EDS analysis revealed that the SB sample distinctly exhibited a robust peak corresponding to its iron content, whereas the AD specimen showed a prominent aluminium peak (Fig. 3c). In addition, the iron-based particles within the SB waste demonstrated the most significant peak in terms of intensity, aligning well with the quantified presence of iron oxide as identified in the XRF analysis (refer to Table 3).

XRF spectrometry was employed to examine the elemental constituents and quantities of metals inherent in the specimens. The compositional assessment of AD, based on weight, indicated that aluminium oxide (Al_2O_3) constituted 61.07 % of the sample, a measure that aligns with the established range (45.39–55.17 %) observed in other AD samples, as documented by Dangtungee et al. (2022). Silicon oxide (SiO_2) was responsible for approximately 11.00 % of the composition, whereas ancillary constituents were also identified. These supplementary elements included Na_2O , Cl, MgO, CaO, K_2O , CuO and Fe_2O_3 .

Regarding SB, the XRF analysis results showed the presence of the iron component (Fe_2O_3), accounting for approximately 32.70 % of its

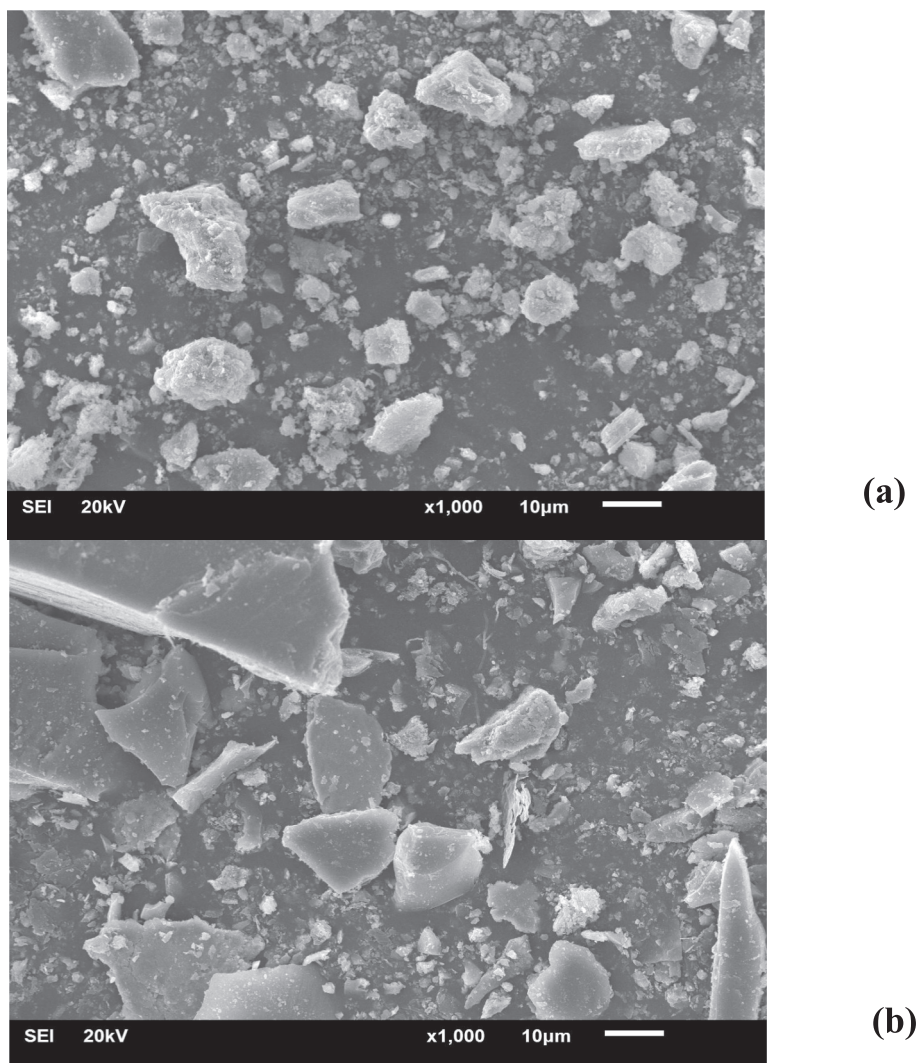


Fig. 3. SEM micrographs with 1000x for a) AD and b) SB; components of elemental analysis using EDS for c) AD and d) SB.

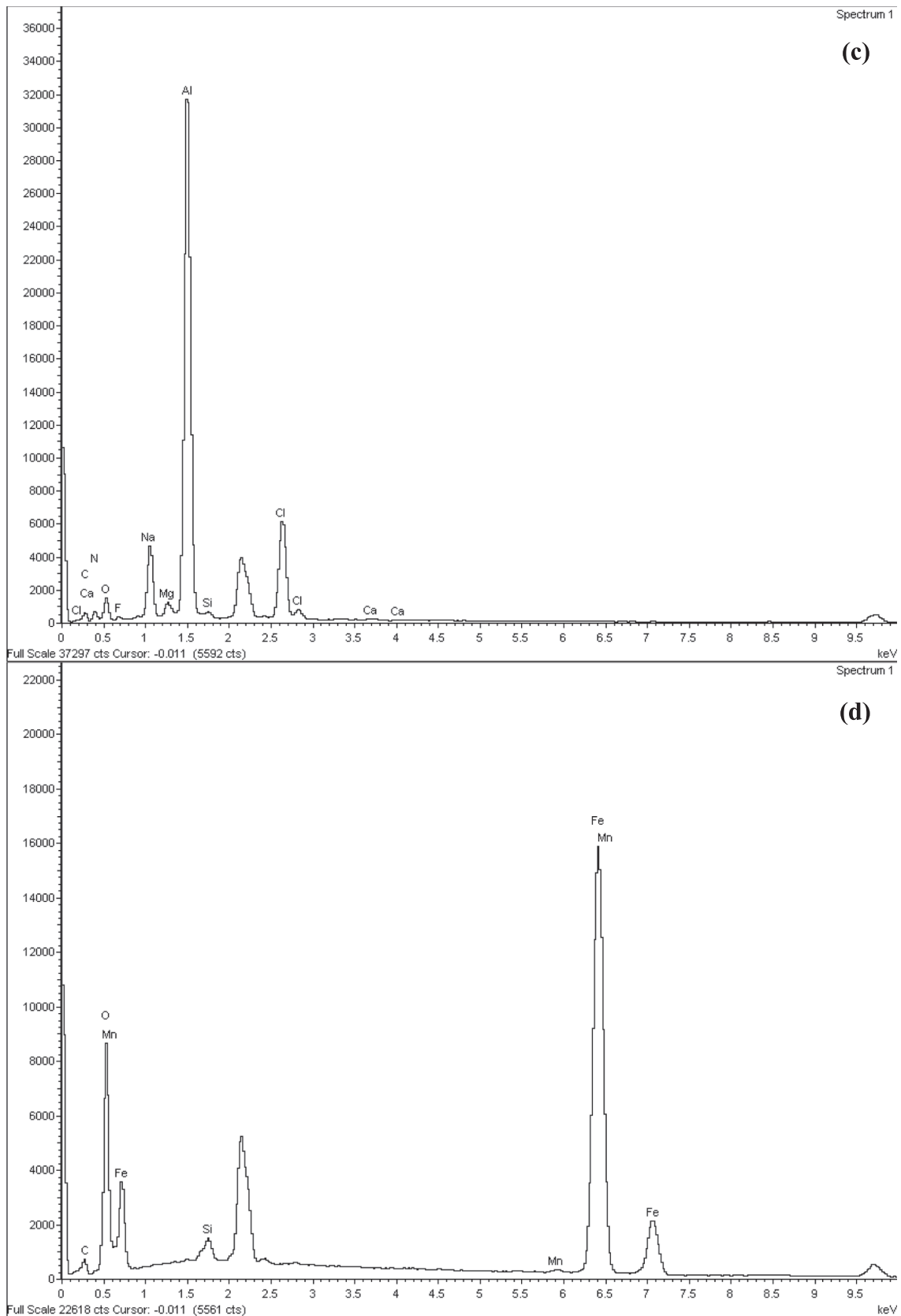


Fig. 3. (continued).

constitution. This iron content played a pivotal role in the manufacturing process of bimetallic particles. Concurrently, it was determined that around 55.30 % of the SB particles comprised SiO_2 , a

composition likely influenced by contamination from the sand mould during the SB procedure, an application wherein SB was administered to the workpiece surface.

Table 3

X-ray fluorescence spectrometry (XRF) results for auto parts manufacturing wastes (AD and SB).

Component	AD: Concentration (wt.%)	SB: Concentration (wt.%)
Al ₂ O ₃	61.07	8.55
SiO ₂	11.00	55.30
Na ₂ O	8.90	0.30
Cl	8.55	0.11
MgO	3.63	0.51
CaO	1.52	0.47
K ₂ O	1.40	0.71
CuO	1.18	0.06
Fe ₂ O ₃	1.15	32.68
SO ₃	0.77	0.15
ZnO	0.54	n/d
MnO	0.22	0.63
Cr ₂ O ₃	0.09	0.18

Numerous studies, including that conducted by Huong et al. (2021), have elucidated the influential role of silica in augmenting COD degradation. This is achieved through the facilitation of robust interactions among catalysts, supporting elements and the substituent iron constituents. Moreover, several researchers have investigated the synthesis and application of diverse iron oxide and silica composites as efficacious Fenton catalysts (Nguyen et al. 2021).

Fig. 4a and 4b display the XRD spectra of AD and SB, respectively. In the AD spectrum, distinct peaks were observed at diffraction angles of 32° (700), 39° (600), 44° (400), 46° (380), 65° (290), and 78° (250). On the other hand, SB exhibited characteristic peaks at 2θ = 32° (700) and 39° (600). Particularly noteworthy is the prominent XRD peak observed in the SB spectrum at 27° (2000). The confirmation of aluminum and iron peaks through EDS analysis corroborated the results obtained from the XRF analysis.

The BET analysis revealed that AD and SB had surface areas of 16.7526 and 3.3233 m² g⁻¹, respectively. Consequently, AD showed approximately five times greater surface area than SB. This discrepancy indicates that during the synthesis of ADSB bimetallic particles, the SB particles were expected to adhere to the surface of AD. The surface area of bimetallic particles supported the absorption of organic compounds in wastewater. The AD and SB samples had average median pore diameters (volume) of 1.903 and 1.909 nm, respectively. However, AD had a small average particle size, measuring 358.15 nm, whereas SB had a particle size of 1805 nm. The results of the BET analysis are shown in Table 4.

3.1.2. Bimetallic particles

Fig. 5 shows the two types of bimetallic particles. The presence of a brown hue in the bimetallic particle morphology could likely be attributed to the interaction with acid during the acid-washing phase, coupled with subsequent heating at 80 °C. In terms of morphology, the ADSB1 sample exhibited a notable concentration of metals, whereas the ADSB2 sample displayed smaller spherical particles than those found in ADSB1. This distinction in particle bimetallic is due to the differing molar ratios employed in the preparation of the bimetallic particles.

In Fig. 6, ADSB1 is evident that the minute quartz constituents have coalesced, with EDS analysis showing prominent peaks corresponding to silica, iron and aluminium. Contrarily, ADSB2 exhibits a configuration marked by numerous sizeable and diffusely scattered quartz particles. The EDS results (Fig. 6d) further indicated the presence of silica and iron as distinguishable components with distinct colours.

The synthesised bimetallic particles underwent XRF analysis to ascertain the weight-based percentage quantities of Al and Fe oxides. The comprehensive outcomes of the XRF analysis are outlined in Table 5. ADSB1 comprised 39.69 % SiO₂, 30.90 % Fe₂O₃ and 16.66 % Al₂O₃, whereas ADSB2 comprised 56.03 % SiO₂, 20.52 % Fe₂O₃ and 16.51 % Al₂O₃. Al₂O₃ served as a catalyst throughout the MAF process using bimetallic particles. Based on this evidence, we assert that bimetallic Fe/Al is likely to exhibit dual functionality, enabling the

simultaneous oxidative and reductive degradation of mixed contaminants (Lien et al., 2019). Nonetheless, it was observed that the degradation of organic contaminants using iron oxides occurred at a comparatively slower pace than the conventional Fenton process. Consequently, it is imperative to further refine the MAF process using ADSB bimetallic particles to augment the efficacy of degradation.

Fig. 7 shows the XRD images for both bimetallic particle samples, ADSB1 and ADSB2. In both instances, the distinctive SB peak emerged at 27° (1000). This peak remained consistent with the observation made when AD and SB were used as substrates in the synthesis of the bimetallic particles. It is a reasonable inference that these bimetallic particles were mainly composed of AD, with SB contributing negligibly to the overall composition.

As shown in Table 6, the BET analysis revealed that the surface areas of the bimetallic particles were 5.1888 ± 0.0079 m² g⁻¹ for ADSB1 and 5.9093 ± 0.0066 m²/g for ADSB2. Both ADSB1 and ADSB2 exhibited similar surface areas. Despite their relatively small surface areas, the particles facilitated adsorption by providing sufficient interfaces for ion-exchange interactions between OH[•] radicals and recalcitrant organic contaminants. This interaction, albeit modestly enhanced by the surface area, is crucial for the breakdown of contaminants. Additionally, the total surface areas of the ADSB1 and ADSB2 particles were 4.270 and 4.804 m² g⁻¹, respectively.

3.2. Synthetic coolant oil wastewater treatment via the MAF process with bimetallic particles

Before applying the MAF process under the specified operating conditions, control sets were investigated to confirm the impact of each parameter on removal efficiency. Four control sets were designed, as shown in Table 7 below.

Without the addition of bimetallic particles into the reactor, the COD and TOC removal efficiencies were 3.05 % and 25.25 %, respectively, under the operating conditions of an initial COD of 3 % v/v, a pH of 9, and an air flow rate of 2 L min⁻¹. This suggests that the aeration system in the wastewater has a minimal effect on removal efficiency. When bimetallic particles were added to the reactor without aeration, while maintaining all other operating conditions the same as in set 1, the COD and TOC removal efficiencies increased to 24.59 % and 52.34 %, respectively. This significant improvement could be attributed to the adsorption of contaminants onto the bimetallic particles. The results indicate that the presence of ADSB particles enhances removal efficiency compared to their absence. In the reactor without bimetallic particles and without aeration, the COD removal was the same as with only aeration. This suggests that no reaction occurred and no radicals were generated. Furthermore, when the initial pH solution was adjusted to an acidic condition, the removal efficiency was notably higher than in the other conditions. This might be due to the acid digesting some easily degradable contents in the wastewater, and the coolant oil wastewater slightly separating into oil and water after the reaction time was complete.

3.2.1. Factors affecting the performance of ADSB bimetallic particles during the MAF process

The 3–5 % v/v of the synthesis coolant oil wastewater contained COD and TOC of 60,000–120,000 and 10,000–40,000 mg L⁻¹, respectively. The efficiency of the MAF process is shown under differently designed operating conditions which are 89.20–97.10 % of COD removal and 94.70–98.00 % of TOC removal as shown in Fig. 8. The most apparent influencing factor is the quantity of bimetallic particles in the reactor. The other significant factors include the initial pH of the wastewater and reaction time. These factors were analysed using the Minitab-19 programme.

In ADSB2, as shown in Fig. 9, the average COD and TOC removal rates were 58.00 % at an initial concentration of 60,000 mg L⁻¹. It achieved the highest COD removal of 96.30 % and TOC removal of

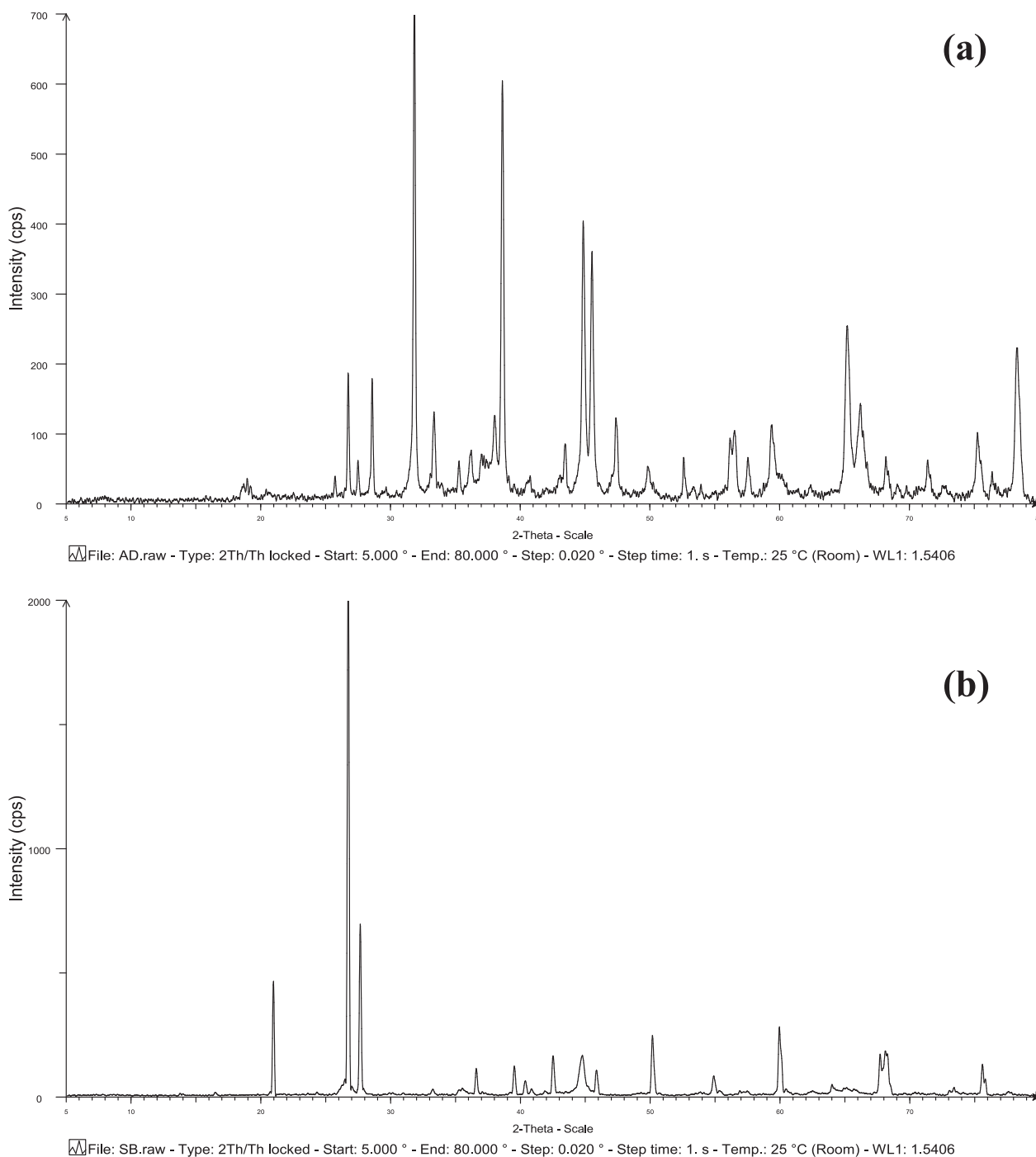


Fig. 4. XRD spectra for a) AD and b) SB.

Table 4
BET analysis of AD and SB particles.

Sample	Surface area (m ² g ⁻¹)	Median pore width (nm)	Avg. particle size (nm)	Molecular cross-sectional area (nm ²)	Total area in the pore (m ² g ⁻¹)	Total volume in the pore (cm ³ g ⁻¹)
AD	16.7526 ± 0.0435	1.903	358.15	0.162	11.32	0.01525
SB	3.3233 ± 0.0209	1.909	1805.00		1.59	0.00127

98.43 %. As the initial wastewater concentration increased, its efficiency slightly decreased. Interestingly, at an initial concentration of 120,000 mg L⁻¹, it achieved COD and TOC removal rates of 77.00 % and 89.69 %, respectively. The overall results might vary based on the elements

present in the bimetallic particles of ADSB1 and ADSB2.

3.2.1.1. Quantity of bimetallic particles. The most apparent influencing factor was the quantity of bimetallic particles in the reactor. Initially, it

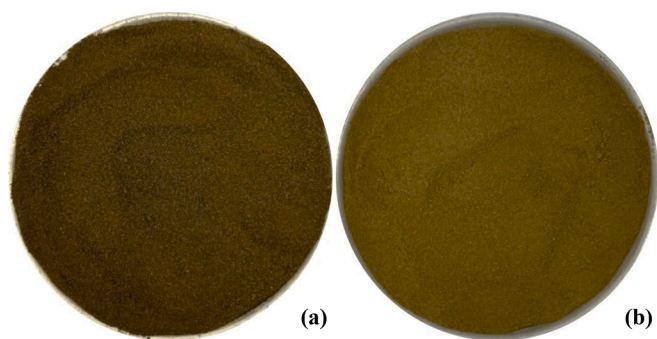


Fig. 5. Bimetallic particles for a) ADSB1 and b) ADSB2.

can be observed that within the range of 0.20–1.00 g, the removal efficiency slightly increases. These ions react with aeration, leading to the generation of radicals in the system. The overall results indicated that a removal efficiency of 95.50 % for COD and 88.80 % for TOC can be achieved at an initial concentration of 3 % v/v. If the initial concentrations are increased, the removal efficiency may decrease due to the higher concentrations of recalcitrant organic pollutants.

For ADSB1, the COD and TOC removal efficiencies ranged from 84.88 % to an impressive 98.02 % when using bimetallic particles in quantities of 0.20–1.0 g, with the same reaction duration of 180 min and initial pH solution. Meanwhile, the ADSB2 particles exerted an effect when bimetallic particles were used in the range of 0.60–1.00 g. Interestingly, the efficiency of COD and TOC degradation demonstrated persistent augmentation with higher quantities of bimetallic particles. Notably, even with an initial COD of 3 % v/v, with TOC at approximately 10,000 mg L⁻¹, the removal efficiency was 97.07 % under the same set of variable conditions.

For ADSB2, favourable outcomes were obtained when 1.00 g of bimetallic particle was used, setting the initial pH at 9 and maintaining an airflow rate of 2.00 L min⁻¹ for 180 min. It can be deduced that the

elevated challenge of eliminating organic pollutants, particularly those characterised by higher COD and TOC values exceeding 120,000 and 40,000 mg L⁻¹, respectively. The significance of aluminium (Al) and iron (Fe) in terms of synergistic effects becomes particularly pronounced when considering the acceleration of ZVI dissolution and the fine-tuning of the Fe (III)/Fe (II) cycling within the framework of ZVI-based Fenton-like reactions. The conversion from Fe (III) to Fe (II) emerges as a critical factor that influences the dynamics of ZVI-based Fenton-like processes, which substantially contributes to their effectiveness (Feng et al., 2023). Therefore, the higher amounts of Fe and Al in the particles exert a positive effect on the efficiency of COD and TOC removal.

The content of iron and aluminium within ADSB played a pivotal role in the MAF process, potentially delivering adequate ions for ion exchange in advanced oxidation process (AOP) reactions. Both the role of iron and the concentration of ferrous ions within the reaction emerged as substantial factors that impact degradation efficiency. An excess concentration of iron ions can detrimentally affect the scavenging process, thereby inducing a decline in overall performance (Wang and Tang, 2021). Elevated concentrations of ferrous ions are normally aligned with an accelerated degradation rate. Nonetheless, an excessive accumulation of unutilised Fe²⁺ ions in the Fenton process can lead to an upsurge in the contents of iron salts and total dissolved solids, exceeding the permissible limits (Wang and Tang, 2021). The use of distinct metal components from bimetallic particles to facilitate a redox cycle akin to a Fenton reaction introduces the possibility of influencing the yield of OH[•] radicals.

3.2.1.2. Initial pH. Fig. 8 shows the performance of ADSB1 bimetallic particles under varying operating conditions. With the initial pH configured at 3, the COD and TOC removal efficiencies achieved values spanning from 77.03 % to 98.54 % for 0.20 g of ADSB1, with a reaction time of 180 min. Nevertheless, the removal efficiencies slightly declined when the initial pH ranged from 6 to 9.

Contrarily, the alternate bimetallic particle variant, ADSB2,

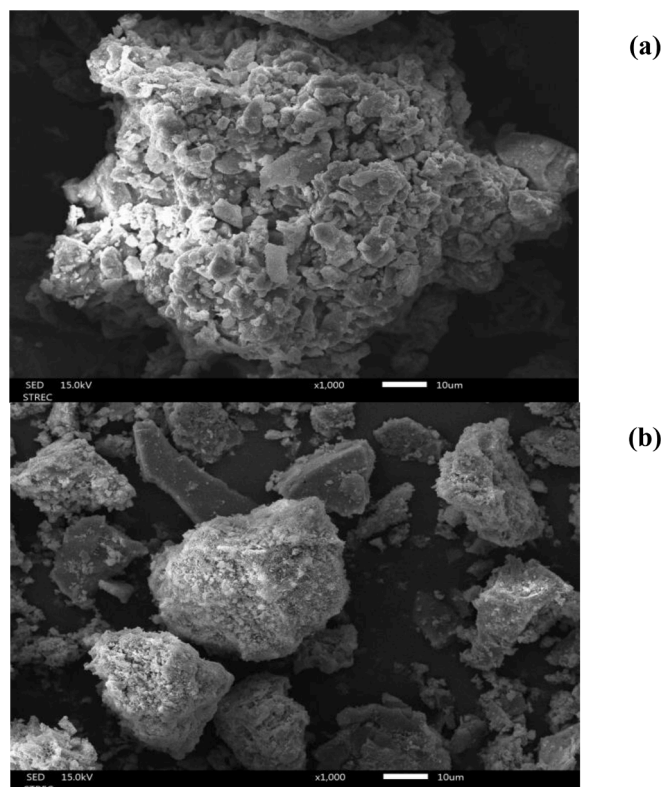


Fig. 6. SEM micrographs with 1000x for a) ADSB1 and b) ADSB2; components of elemental analysis using EDS for c) ADSB1 and d) ADSB2.

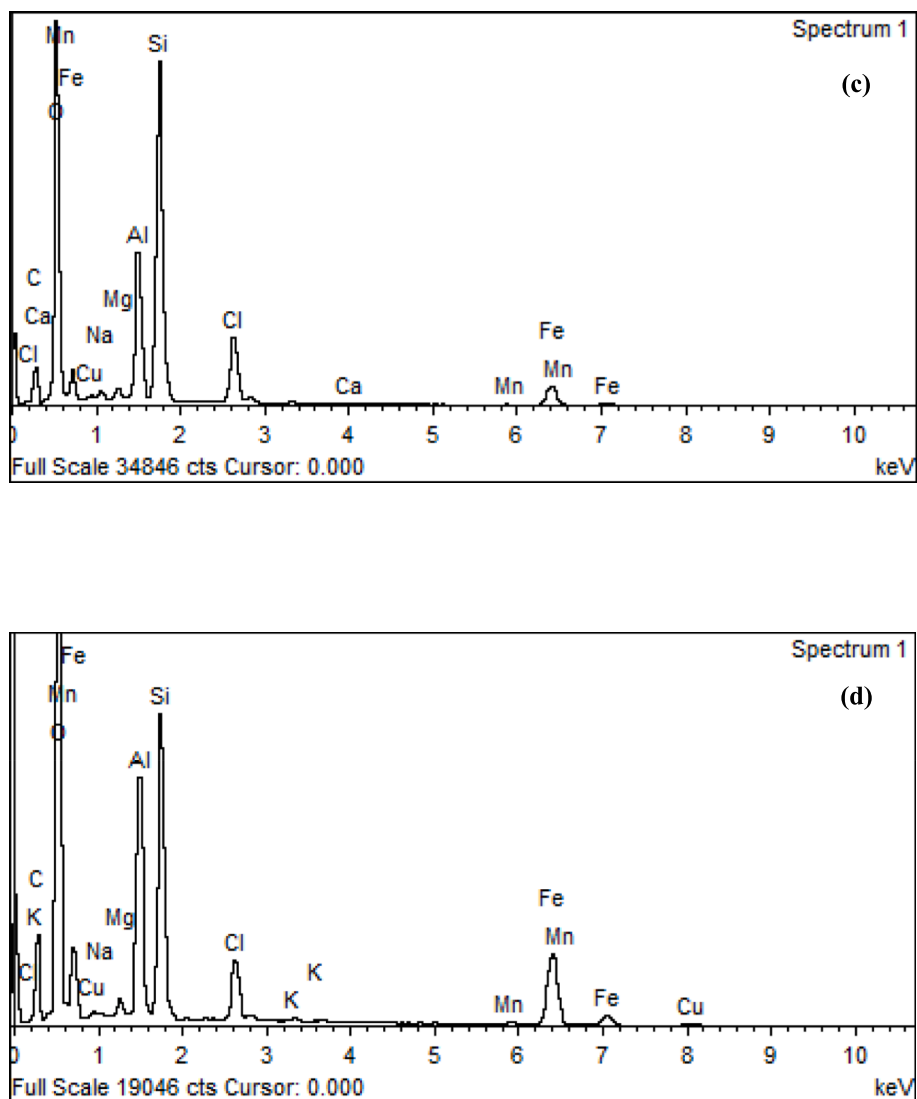


Fig. 6. (continued).

Table 5

XRF analysis of the synthetic bimetallic particles.

Component	ADSB1 concentration (wt.%)	ADSB2 concentration (wt.%)
SiO ₂	39.69	56.03
Fe ₂ O ₃	30.90	20.52
Al ₂ O ₃	16.66	16.51
Cl	7.97	2.70
CuO	0.96	0.47
MgO	0.76	0.93
K ₂ O	0.66	0.78
MnO	0.59	0.50
CaO	0.53	0.30
Na ₂ O	0.48	0.44
TiO ₂	0.24	0.33
Cr ₂ O ₃	0.19	0.16
SO ₃	0.15	0.15
ZnO	0.11	0.04
P ₂ O ₅	0.05	0.04
ZrO ₂	0.05	0.04
SrO	0.02	0.01

exhibited a relatively lower efficiency, achieving only 56.01 % under identical experimental conditions. The removal efficiency for 0.20 g of bimetallic particles declined when adhering to the original wastewater pH, which was approximately 9. Conversely, adjustment of the initial

wastewater pH to acidic conditions (pH 3) led to increased efficiency compared with the results obtained at pH 9.

Both ADSB particles exhibited the same trend, which is acidic pH is better than the basic pH value. As evidenced by numerous researchers, the pH of the solution plays a pivotal role in AOPs that involve the use of catalysts capable of activating molecular oxygen, leading to the generation of reactive oxygen species (ROS) within the solution. In AOPs, lower pH values result in the liberation of more H⁺ ions, subsequently inducing an increased generation of ROS (Rubio-Clemente et al., 2015). For the Fenton reaction, the optimal pH range was generally 2.8–3.0, contingent upon the specific target pollutants undergoing treatment (Li et al., 2020). Under acidic conditions, the generation of free Fe²⁺ and Fe³⁺ ions in the system, crucial for the iron regeneration cycle, can be influenced (Wang and Tang, 2021). Conversely, in cases where the pH is 4.00 or above, aluminium hydroxide may precipitate on the surface catalyst, impeding ROS production (Rubio-Clemente et al., 2015). Consequently, pH stands as a significant constraining factor that substantially shapes the efficacy of the Fenton reaction (Wang and Tang, 2021).

3.2.1.3. Airflow rate. The effects of airflow rates were operated by 1.00, 1.50 and 2.00 L min⁻¹ to observe the removal results. The MAF results indicated that the airflow rate did not consistently adhere to the same

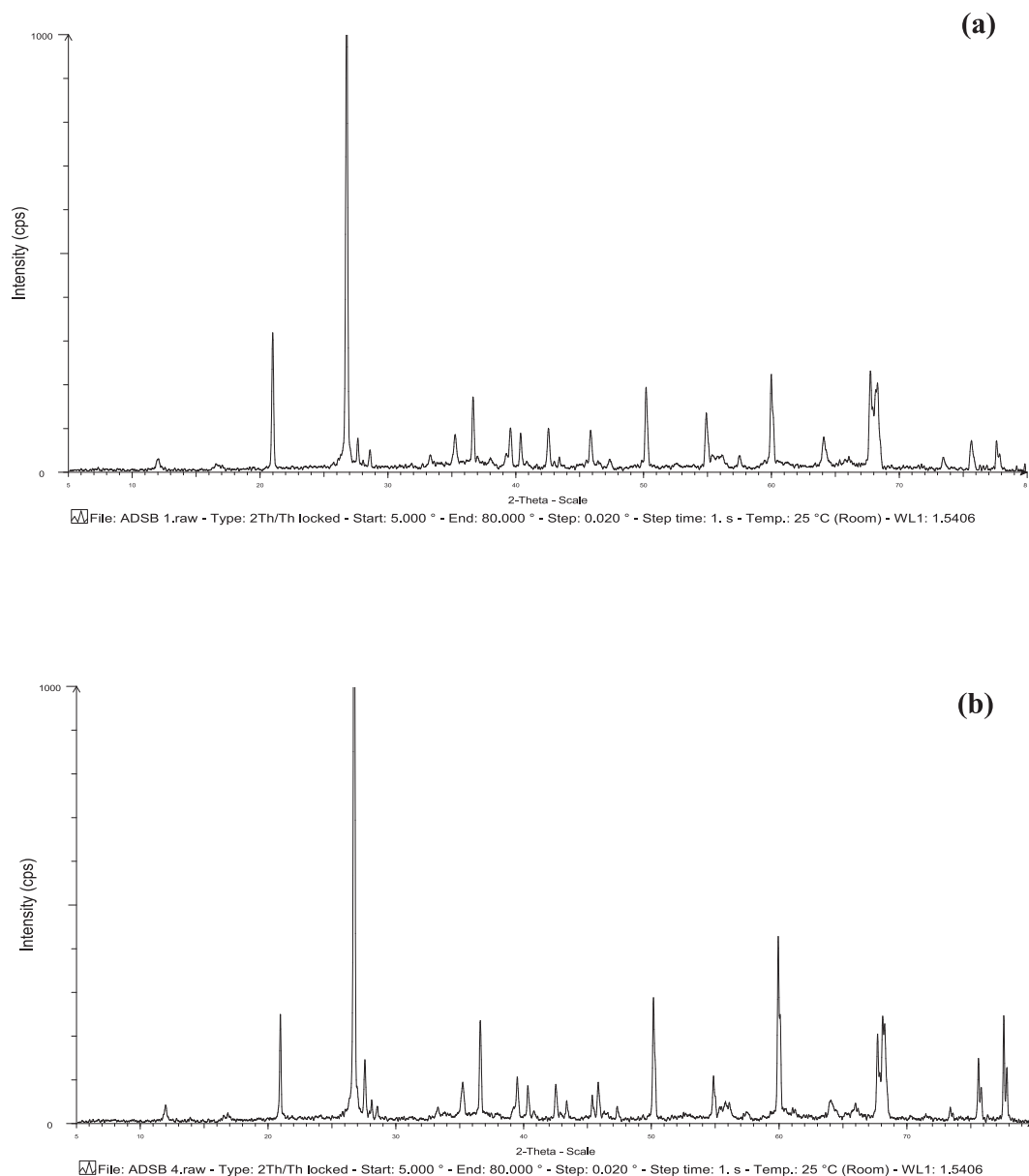


Fig. 7. XRD of bimetallic particles for a) ADSB1 and b) ADSB2.

Table 6
BET bimetallic particles.

Sample	Surface area ($\text{m}^2 \text{g}^{-1}$)	Median pore width (nm)	Avg. particle size (nm)	Molecular cross-sectional area (nm^2)	Total area in the pore ($\text{m}^2 \text{g}^{-1}$)	Total volume in the pore ($\text{cm}^3 \text{g}^{-1}$)
ADSB1	5.1888 \pm 0.0079	1.9066	1156	0.162	4.270	0.01085
ADSB2	5.9093 \pm 0.0066		1015		4.804	0.00639

pattern of influencing the removal efficiency. Instead, the outcomes were more profoundly influenced by the quantity of bimetallic particles used and the duration of the reaction. Consequently, the airflow rate variations had no considerable impact on the removal efficiencies of

COD and TOC. Overall, the removal efficiency exhibited substantial variability, with values fluctuating depending on the aforementioned conditions. The airflow rate in the MAF process was slightly impacted by the removal when the results were analysed using Minitab-19 for a concise summary.

In the MAF process, the bimetallic particles infused the reactor with elevated concentrations of metal ions, and these Fe^{2+} and Al^{3+} ions engaged in interactions with the specified pollutants in the study. The reaction mechanism exerted a cascading effect with aluminium dissolving into aluminium ions, as expressed in the following equations (Chen et al., 2008, Lien et al., 2019, Saber et al., 2014, Xiong et al., 2015, Yuan et al., 2016, Li et al., 2020, Babuponnusami and Muthukumar, 2014):



Table 7a

Control Sets for the MAF Process with Synthetic Coolant Oil Wastewater.

Control set	Wastewater concentration (% v/v)	Bimetallic quantity (g)	Initial wastewater pH	Time (min)	Airflow rate (L min ⁻¹)	% COD removal	TOC removal
1	3	0	9	180	2	3.05	25.25
2	3	1	9	180	0	24.59	52.34
3	3	0	9	180	0	6.64	27.25
4	3	0	2	180	0	40.61	54.89

Table 7b

Prediction of response optimization for the percentage removal of COD and TOC in the MAF process under variable conditions.

Variable	COD at 95 % removal efficiency		TOC at 95 % removal efficiency	
	ADSB1	ADSB2	ADSB1	ADSB2
Bimetallic quantity (g)	1.0	0.8	1.0	1.0
Initial wastewater pH	9	9	3	9
Time (min)	36	180	94	180
Airflow rate (L min ⁻¹)	1	2	2	2
Wastewater concentration (% v/v)	3	3	3	3



The presence of dissolved oxygen (DO) within the reaction solution substantially contributed to the increased generation of H₂O₂, thereby amplifying the oxidation potential of the Fe⁰/air process. Yuan et al. (2016) conducted a comprehensive investigation on the COD removal efficiencies of ammunition wastewater using the Fe⁰/air process under varying airflow rates (0.00, 0.50, 1.00 and 1.50 L min⁻¹). As a result, the efficiency of COD removal rapidly increased with the increase in the airflow rate (Xiong et al., 2015). The Fenton reaction assumes an importance within the MAF reactor, as it disrupts ion exchange in the wastewater during the reaction time, thereby facilitating the degradation of complex organic compounds that would otherwise be formidable to decompose.

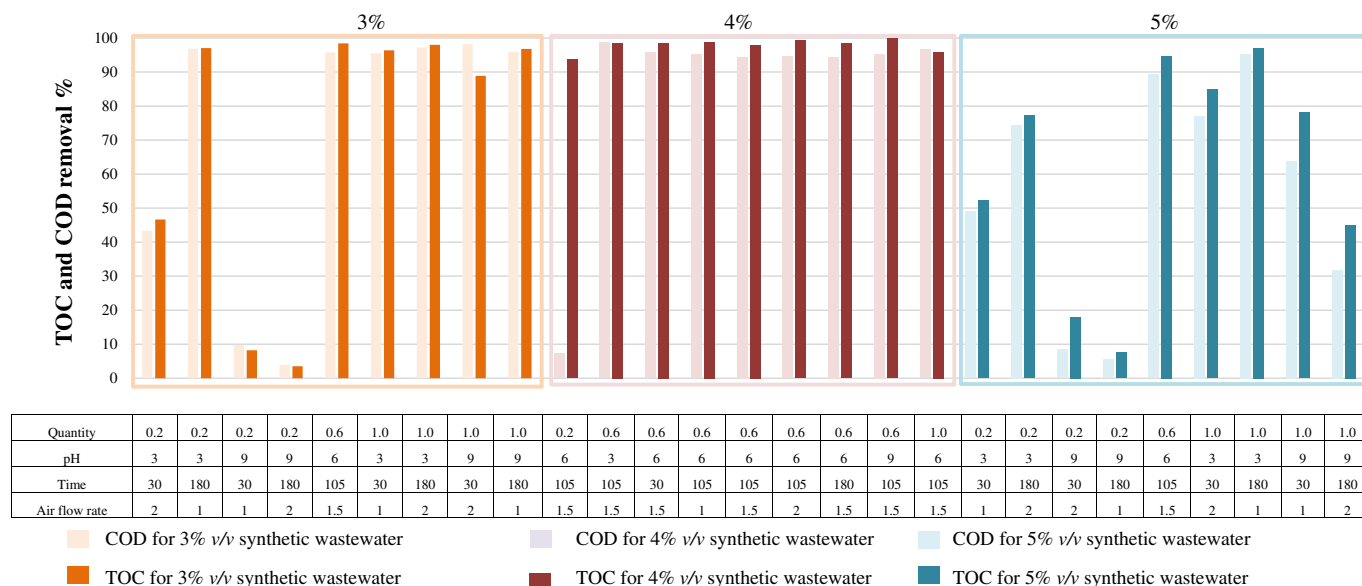
The preliminary test data analysis revealed that the DO levels in the solution maintained a consistent pattern. As the reaction time progressed, the DO content in the solutions increased to 2.00 mg L⁻¹. After the completion of the reaction, the majority of DO values stabilised around 5.00 mg L⁻¹, regardless of the distinct airflow rates used.

3.2.1.4. Reaction time. The parameter of the reaction time substantially influenced the efficacy of COD and TOC removal in the MAF reaction. For a dosage of 0.20 g of ADSB1, the COD removal rate stood at approximately 46.65 % after a 30-min reaction time, whereas it notably escalated to 97.03 % when the reaction time was extended to 180 min. Conversely, ADSB2 achieved COD and TOC removal rates of 98.43 % and 96.30 %, respectively, under identical conditions of pH 9 and an airflow rate of 2.00 L min⁻¹ maintained for 180 min. The duration of the reaction process is acknowledged to have a direct correlation with the degradation of targeted pollutants (Nguyen et al., 2021). In the conventional Fenton reaction, a reaction time of approximately 60 min is typically optimized to achieve removal efficiencies spanning from 60.00 % to 99.00 % (Nguyen et al., 2021, Ghime and Ghosh, 2017). However, the specific reaction duration might fluctuate based on the inherent nature of the degradation target.

Hence, the reaction time stands as another pivotal parameter within the MAF process, exerting a pronounced influence on the removal efficiency. It is contingent upon the distinctive characteristics, reactant concentrations and specific wastewater treatment methodology. The data presented in Figs. 8 and 9 indicate that the removal efficiencies of both COD and TOC are subject to the direct impact of the reaction time. The peak removal efficiencies emerged at a reaction time of 180 min for both COD and TOC.

3.2.2. CCD analysis of COD and TOC removal efficiency

3.2.2.1. 3D surface plots of the two-parameter-interaction effects. All experiment was conducted, and data on COD and TOC removal were gathered and subsequently analysed using Minitab-19. This software was used to generate statistical data by applying the DOE technique with CCD. Fig. 10 shows 3D surface plots that vividly depict the interactive effects of two key parameters, namely, the quantity of bimetallic particles and the initial pH, on the removal of COD and TOC from ADSB1. As

**Fig. 8.** Removal efficiency of the MAF process with ADSB1 for synthetic coolant oil wastewater.

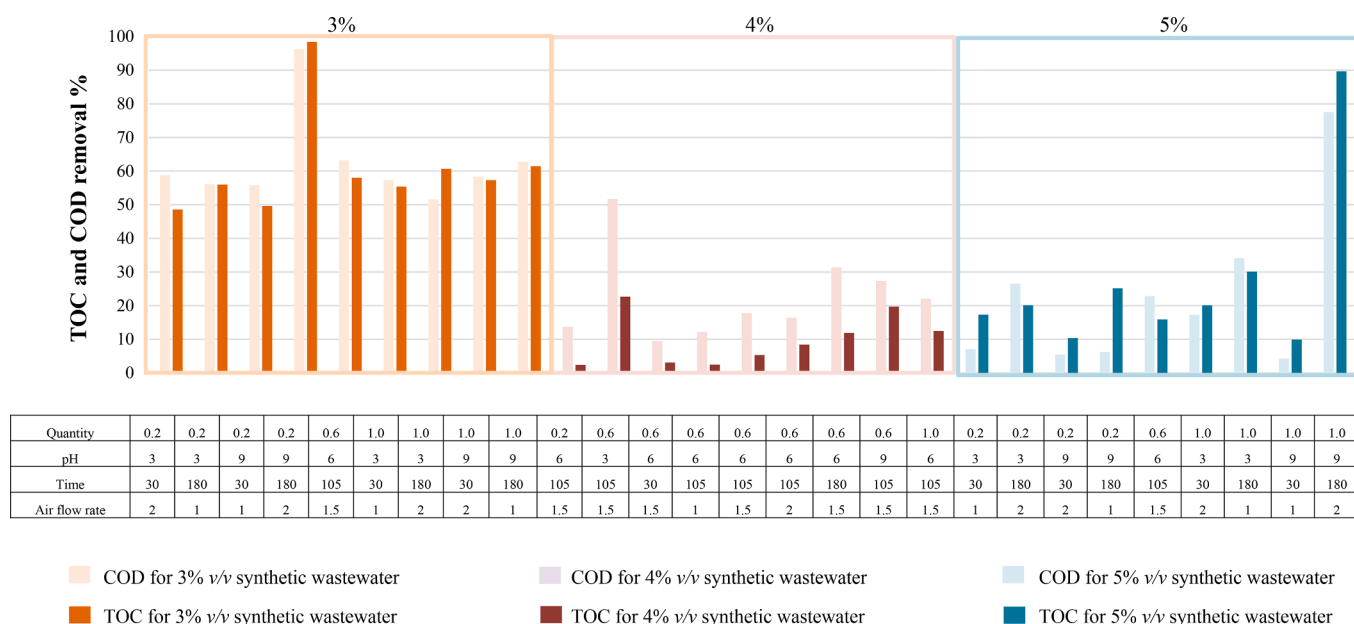


Fig. 9. Removal efficiency of the MAF process with ADSB2 for synthetic coolant oil wastewater.

delineated in the graphical representation, an escalation in the proportion of bimetallic particles culminates in an overall augmentation of efficiency. The optimal bimetallic particle concentration falls within the range of 0.60–1.00 g, taking into account the metal ions generated during the COD and TOC reduction. The versatility of the MAF process is emphasised by its efficacy over a broad spectrum of pH values, spanning from 3 to 9, thereby circumventing the need for pH adjustments while upholding commendable removal efficiency. The interrelation between the pH level and quantity of ADSB1 bimetallic particles is depicted in the COD removal results in Fig. 10a. COD removal efficiency ranging from 80 % to 95 % was achieved within the particle quantity range of 0.40–0.95 g by adjusting the pH value from an acidic condition to nearly neutral (pH 6–8). Over a range of these conditions, the scavenging of Fe or Al competes to react with OH radicals instead of degrading organic matter.

In Fig. 10b, efficacious TOC removal was achievable within the range of 0.25–1.00 g of bimetallic particles, accompanied by an extended pH range of 3–9. This notable enhancement exceeds the more restricted pH spectrum characteristic of the conventional Fenton reaction. In addition, Fig. 10c shows the outcomes for the ADSB2 sample, elucidating the dynamic relationship between the reaction time and the concentration of synthetic coolant oil wastewater. In the context of a 3 % concentration (60,000 mg L⁻¹), a COD removal efficiency of 60 % was achieved within a temporal frame of 100–180 min. Notably, the trend for TOC removal portrayed an opposing trajectory compared with the initial COD content of both the AD and SB ratios of the bimetallic particles. This interesting finding may hint at increased resilience to degradation under the current conditions, possibly stemming from the distinct attributes of the ADSB2 sample.

3.2.2.2. Prediction of response optimization. Analysis using Minitab-19 revealed the conditions for achieving approximately 90–95 % removal efficiency of organic pollutants, specifically COD. These optimal conditions were established for a COD concentration of 90,000 mg L⁻¹ using 0.20 g of ADSB2, setting an initial pH value of 9 and maintaining a constant airflow rate of 2 L min⁻¹ over a 180-min period. The comprehensive summary of response optimization outcomes, emphasising the percentage removal of TOC within the MAF process under various conditions, is presented in Table 7. The dataset mainly explores

the parameter range of 0.80–1.00 g for bimetallic particles, identified as the optimal dosage for ensuring a substantial presence of iron and aluminium in both ADSB bimetallic specimens.

Concerning COD removal, the computational model highlighted the appropriateness of a pH value of 9 when addressing coolant oil wastewater at a concentration of 3 % v/v. In addition, the findings indicated the feasibility of using a slightly increased quantity of bimetallic particles as a strategy to reduce reaction time, as shown in Table 7. In the quest to achieve removal levels of 95 % for both COD and TOC, the predictions recommend the utilisation of 1.00 g of ADSB, coupled with an airflow rate of 2.0 L min⁻¹ and an initial concentration of 3 % v/v. Notably, for the ADSB1 sample, achieving elevated efficiency levels required an initial pH modification over 94 min within an acidic environment. Conversely, achieving comparable high removal efficiencies required no pH adjustments when the reaction duration was extended to 180 min.

To achieve accurate forecasts of the removal efficiency parameters in the MAF process using distinct ADSB ratios in bimetallic particles, a set of regression equations was implemented. These equations were categorised into four segments encompassing COD and TOC equations for both ADSB1 and ADSB2. Each of these equations played a pivotal role in predicting the removal efficiency within the MAF process batch with bimetallic particles, as expressed in Equations 14–17.

$$\begin{aligned} \text{COD}_{\text{ADSB1}} = & -26 + 411.6A - 7.5B + 0.678C - 29D + 11.9E \\ & - 257.7A^2 + 0.427B^2 + 0.00034C^2 + 6.7D^2 - 0.68E^2 \\ & + 8.36AB - 0.176AC - 4.8AD - 16.00AE - 0.0395BC \\ & + 0.49BD - 1.27BE - 0.1587CD - 0.0319CE + 4.20DE \end{aligned} \quad (14)$$

$$\begin{aligned} \text{COD}_{\text{ADSB2}} = & 525.6 - 41.2A - 28.67B - 0.418C + 55.0D - 202.9E \\ & - 30.5A^2 + 1.863B^2 - 0.000416C^2 - 33.8D^2 + 20.25E^2 \\ & + 1.42AB + 0.0643AC - 4.87AD + 19.51AE \\ & + 0.02532BC + 4.54BD - 0.849BE + 0.1292CD \\ & + 0.0616CE + 5.27DE \end{aligned} \quad (15)$$

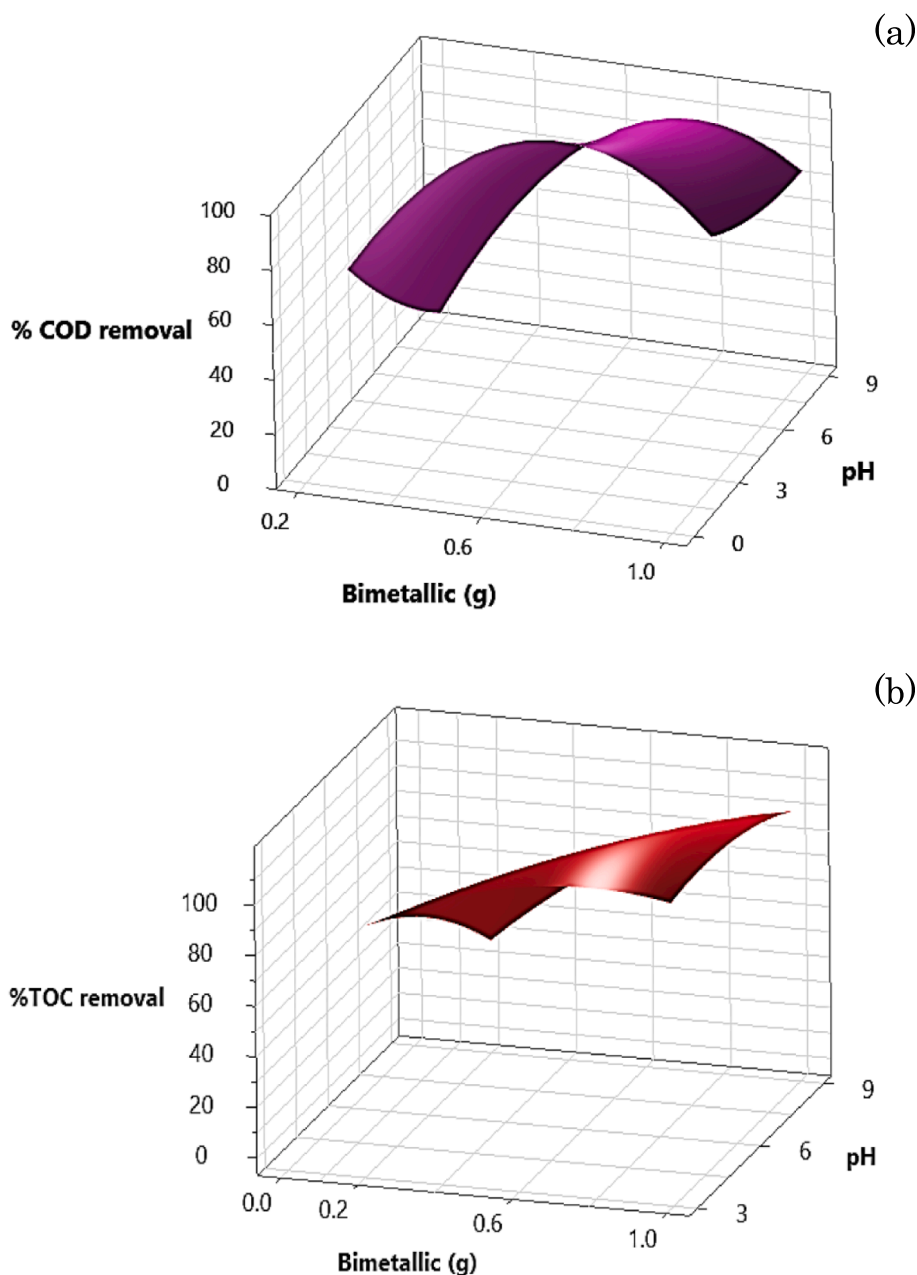


Fig. 10. 3D-surface plots of the two-parameter-interaction effects of the amount of bimetallic particle and initial pH on (a) COD removal, (b) TOC removal of bimetallic particle ADSB1. 3D-surface plots of the two-parameter-interaction effects of the amount of bimetallic particle and initial pH on (c) COD removal and (d) TOC removal of bimetallic particle ADSB2.

$$\begin{aligned}
 \text{TOC}_{\text{ADSB1}} = & -193 + 159.3A + 3.4B + 1.012C + 66D + 74.6E \\
 & - 68.6A^2 - 0.72B^2 - 0.00129C^2 - 26.7D^2 - 9.19E^2 \\
 & + 8.76AB - 0.149AC - 10.0AD - 11.66AE - 0.0360BC \\
 & + 0.03BD - 0.46BE - 0.1301CD - 0.0512CE + 6.47DE
 \end{aligned}
 \tag{16}$$

A: Bimetallic particles (g)
 B: pH
 C: Reaction time (min)
 D: Airflow rate (L min^{-1})
 E: Wastewater concentration (% v/v)

$$\begin{aligned}
 \text{TOC}_{\text{ADSB2}} = & 679.6 - 71.6A - 27.00B - 0.442C - 15.7D - 262.3E \\
 & - 5.2A^2 + 1.437B^2 - 0.000135C^2 - 1.3D^2 + 28.71E^2 \\
 & + 0.55AB + 0.0528AC + 12.96AD + 14.79AE \\
 & + 0.03389BC + 4.956BD + 0.026BE + 0.1536CD \\
 & + 0.0349CE + 1.90DE
 \end{aligned}
 \tag{17}$$

3.2.3. Proposed fundamental mechanisms for the MAF process with bimetallic particles

In line with the utilisation of ADSB in the MAF process, the intricate mechanism of electron transfer is elucidated through diverse processes (Xiong et al., 2015). The sequence commences with the corrosion of ZVAL, leading to the emission of electrons and aluminium ions (Al^{3+}) and subsequently embarking upon the reduction of molecular oxygen.

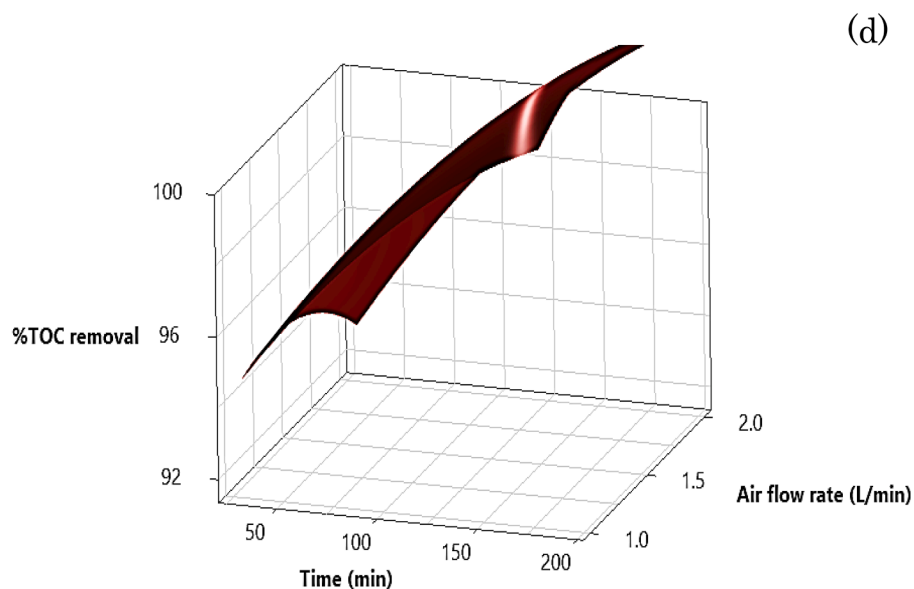
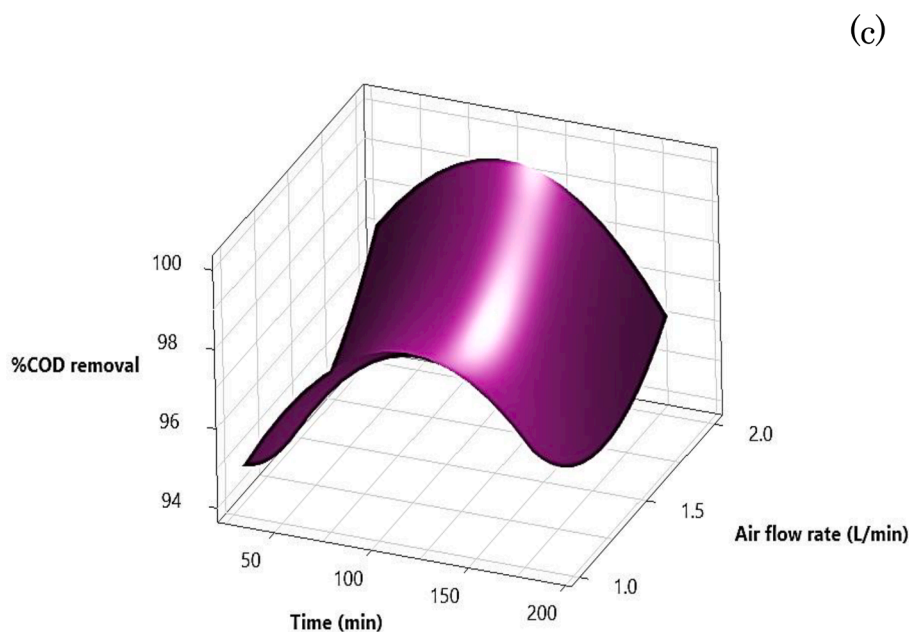


Fig. 10. (continued).

Then, the swift disproportionation of HO_2 culminates in the generation of H_2O_2 . Consequently, ZVAL, in its turn, relinquishes electrons, channelling them towards H_2O_2 , thereby inducing the production of OH^\cdot radicals. This electron transfer culminates with H_2O and H^+ ions in solution vying for electrons, resulting in hydrogen discharge. Correspondingly, iron compounds partake in the same procession as aluminium. The reactions are eloquently captured in Equations (9)–(13), outlining the organic compound degradation orchestrated by the MAF reaction. The majority of iron and aluminium are engaged in a dance with hydrogen, introduced through an aeration system. The ensuing outcome is the genesis of H_2O_2 , which harmonises with organic compounds. This intricate interplay may subsequently metamorphose these compounds into CO_2 and H_2O , emerging as benign by-products in the final step. The holistic panorama of these reactions is masterfully portrayed in Fig. 11. The vitality of aeration feeding within the precincts of the MAF process, which is attributable to the presence of Fe^0/Al^0 within the ADSB bimetallic configuration, highlights its role in engendering O_2 for oxidation. This, in turn, engenders Fe^{2+} and H_2O_2 .

Subsequently, the bimetallic particles engage in the reduction of Fe^{3+} to Fe^{2+} . Ultimately, these overarching reactions harmonise with the Fenton mechanisms, thereby fostering the concurrent degradation of recalcitrant pollutants within wastewater (Zhang et al., 2016).

3.3. Effect of a scavenger

Using the targeted 95 % removal efficiency as a benchmark, the design of the MAF batch experiment was meticulously tailored in accordance with the outlined parameters. In the context of the scavenger analysis experiment, isopropyl alcohol (IPA) was selected as the organic compound owing to its rapid reactivity with OH^\cdot radicals within the Fenton reaction.

Fig. 12 shows an illustrative platform for portraying the outcomes gleaned from the ADSB1 and ADSB2 experiments. Within the ambit of conditions outlined under headings E and F, ADSB1 demonstrated a removal efficiency ranging from 87.50 % to 98.18 % for both COD and TOC. These experimental settings entailed the utilisation of 1.00 g of

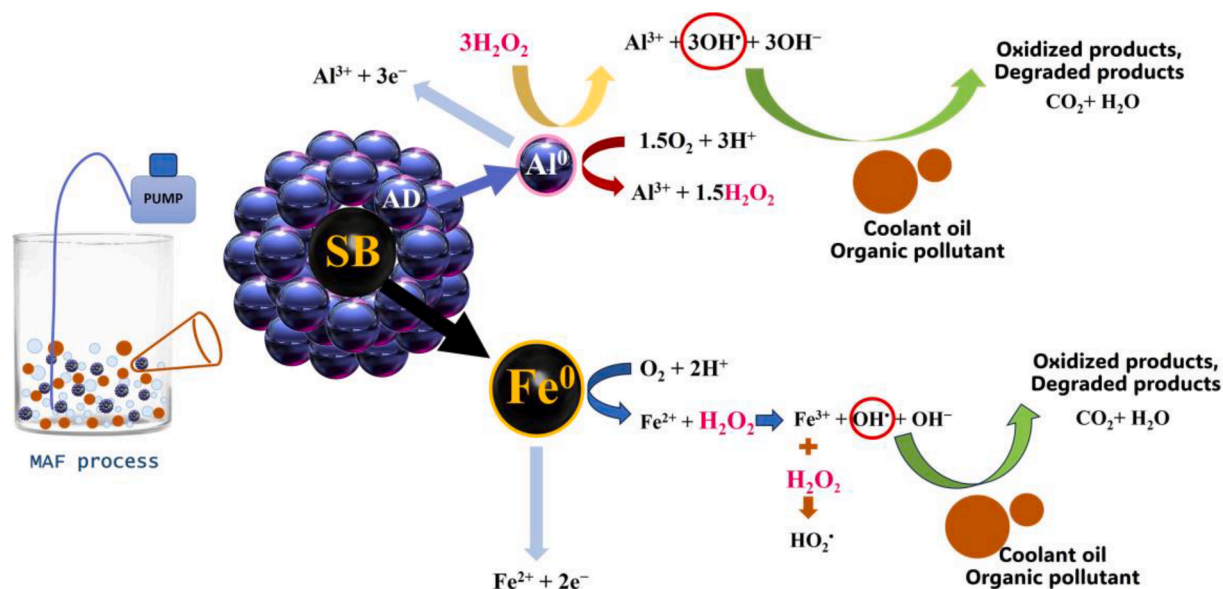


Fig. 11. Proposed fundamental mechanisms for the MAF process with bimetallic particles (modified from Lien et al. (2019), Fu et al. (2022)).

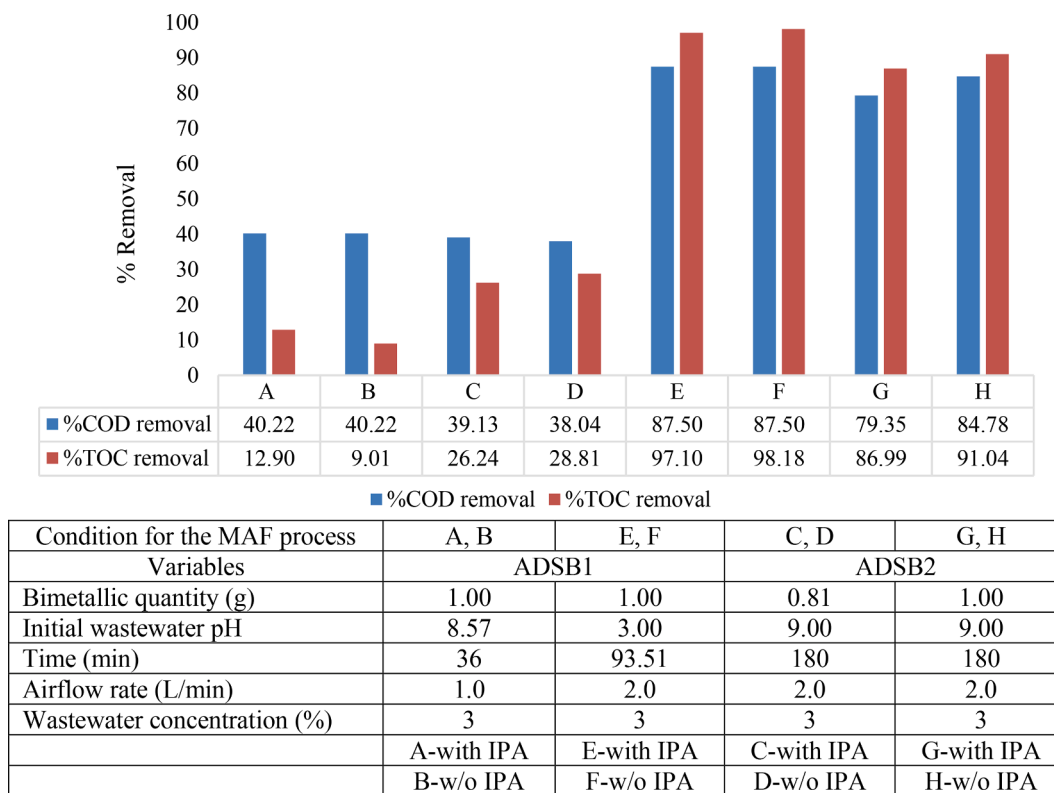


Fig. 12. Effect of isopropyl alcohol (IPA) on COD and TOC removal efficiency.

ADSB1, an initial pH value of 3, an airflow rate of 2.0 L min⁻¹ and an entire reaction span approximating 94 min. Conversely, ADSB2 bimetallic particles, when assimilated into the MAF process, exhibited a removal efficiency spanning from 79.35 % to 91.04 % for COD and TOC under conditions marked by headings G and H. These parameters mandated the application of 1.00 g of ADSB2, a dynamic initial pH range spanning from 3 to 9 and an airflow rate of 2.0 L min⁻¹, synchronised with a reaction period ranging from 93 to 180 min. Notably, the batches infused with IPA as a scavenger additive yielded marginally moderated outcomes compared with their no scavenger counterparts.

Clearly, the pivotal factors contributing to the effectiveness of the MAF process encompass the quantity of bimetallic particles and the temporal dimensions of the reaction. As the results expounded under headings A and B for ADSB1 indicate, abbreviated reaction durations are directly proportional to relatively subdued removal efficiency. Conversely, within the context of headings C and D for ADSB2, a reduced proportion of bimetallic particles wielded a tangible impact on performance, even when encountering identical reaction durations. The efficiency in expelling pollutants experienced marginal tapering due to the substitution of organic pollutants with IPA within the synthesised

coolant oil wastewater. Consequently, within specific batches enriched with IPA, the efficiency of the MAF process exhibited a slight decline compared with their IPA-absent counterparts. Interestingly, a subset of batches demonstrated immunity to the magnitude of IPA introduced, suggesting the possibility of alternative organic pollutants within the wastewater engaging with OH[•] radicals, avoiding the influence of IPA.

4. Conclusion

The research presented here demonstrates the innovative utilization of waste materials, specifically aluminium dross (AD) and shot blast (SB) residues from auto parts manufacturing, to synthesize ADSB bimetallic particles with varying compositions. These bimetallic particles, ADSB1 (AD ratio of 1:1) and ADSB2 (AD ratio of 2:1), were employed in the MAF process to effectively reduce high COD (60,000–120,000 mg L⁻¹) and TOC (10,000–40,000 mg L⁻¹) levels in coolant oil wastewater.

By leveraging the capabilities of Minitab-19 for experimental design, we accurately predicted removal efficiencies by finely adjusting operational conditions to achieve the desired target percentages. For ADSB1, achieving a COD and TOC removal efficiency of 95 % required specific conditions: 1.00 g of bimetallic particles, an initial pH of 3, a reaction time of approximately 94 min, and an airflow rate of 2.0 L min⁻¹. In contrast, ADSB2 required 1.00 g of bimetallic particles, an initial pH of 9, a reaction time of approximately 180 min, and an airflow rate of 2.0 L min⁻¹ to achieve the same removal efficiency.

Despite its shorter reaction duration and time limitations, ADSB1 was selected as the bimetallic particle for the reactor. Conversely, ADSB2 is recommended for situations where the initial wastewater pH limits the amount of chemicals required for synthetic wastewater preparation. Both ADSB bimetallic particles demonstrated the synergistic prowess of iron and aluminium, delivering robust removal efficiencies across a wide range of initial wastewater pH values.

It is prudent for researchers to adapt and apply these conditions extrapolated from the forecasted removal efficiency values. Furthermore, by fine-tuning the utilization of waste materials from auto parts manufacturing, this study highlights the potential to enhance and fortify the MAF process.

Funding

This work was supported by the 100th Anniversary Chulalongkorn University Fund for Doctoral Scholarship and the 90th Anniversary of Chulalongkorn University Fund Ratchadaphiseksomphot Endowment Fund. The authors are grateful for the scholarship from Programmes in Hazardous Substance and Environmental Management, Graduate School, Chulalongkorn University, Bangkok, Thailand.

CRediT authorship contribution statement

Hathaichanok Suannuch: Writing – review & editing, Writing – original draft, Methodology, Investigation, Formal analysis. **Vorapot Kanokkantapong:** Writing – review & editing, Validation, Supervision, Project administration, Investigation, Funding acquisition, Data curation, Conceptualization. **Jatuwat Sangsanont:** Writing – review & editing, Supervision, Data curation, Conceptualization.

Declaration of competing interest

The authors declare that they have no known competing financial interests or personal relationships that could have appeared to influence the work reported in this paper.

Acknowledgements

The authors wish to thank all supporters including the research was supported by the 100th Anniversary Chulalongkorn University Fund for Doctoral Scholarship and the 90th Anniversary of Chulalongkorn University Fund Ratchadaphiseksomphot Endowment Fund. The authors are grateful for the scholarship from Programmes in Hazardous Substance and Environmental Management, Graduate School of Chulalongkorn University, Bangkok, Thailand. Furthermore, I would like to thank the laboratory support from the Centre of Excellence on Hazardous Substance Management, Bangkok, Thailand, Department of Environmental Science, Faculty of Science, Chulalongkorn University, Bangkok, Thailand for my support experiment room and convenient.

References

- Amin, M.M., Mofrad, M.M.G., Pourzamani, H., Sebaradar, S.M., Ebrahim, K., 2017. Treatment of industrial wastewater contaminated with recalcitrant metal working fluids by the photo-Fenton process as post-treatment for DAF. *J. Ind. Eng. Chem.* 45, 412–420.
- Babuponnusami, A., Muthukumar, K., 2014. A review on Fenton and improvements to the Fenton process for wastewater treatment. *J. Environ. Chem. Eng.* 2 (1), 557–572.
- Chen, L.H., Huang, C.C., Lien, H.L., 2008. Bimetallic iron–aluminum particles for dechlorination of carbon tetrachloride. *Chemosphere* 73 (5), 692–697.
- Dangtungee, R., Vatcharakajon, P., Techawinyutham, L., 2022. Aluminium dross neutralization and its application as plant fertilizer. *Mater. Today: Proc.* 52, 2420–2426.
- Feng, C., Zhang, H., Ren, Y., Luo, M., Yu, S., Xiong, Z., Liu, Y., Zhou, P., ai, B., 2023. Enhancing zerovalent iron-based Fenton-like chemistry by copper sulfide: Insight into the active sites for sustainable Fe (II) supply. *J. Hazard. Mater.*, 452, 131355.
- Fu, W., Yi, J., Cheng, M., Liu, Y., Zhang, G., Li, L., Du, L., Li, B., Wang, G., Yang, X., 2022. When bimetallic oxides and their complexes meet Fenton-like process. *J. Hazard. Mater.* 424, 127419.
- Ghime, D., Ghosh, P., 2017. Heterogeneous Fenton degradation of oxalic acid by using silica supported iron catalysts prepared from raw rice husk. *J. Water Process Eng.* 19, 156–163.
- Lermen, R.T., Prauchner, M.B., Silva, R.D.A., Bonsembiante, F.T., 2020. Using wastes from the process of blasting with steel shot to make a radiation shield in mortar. *Sustainability* 12 (16), 6674.
- Li, D., Zheng, T., Liu, Y., Hou, D., Yao, K.K., Zhang, W., Song, H., He, H., Shi, W., Wang, Lu., Ma, J., 2020. A novel Electro-Fenton process characterized by aeration from inside a graphite felt electrode with enhanced electro generation of H₂O₂ and cycle of Fe³⁺/Fe²⁺. *J. Hazard. Mater.* 396, 122591.
- Lien, H.L., Yu, C.H., Kamali, S., Sahu, R.S., 2019. Bimetallic Fe/Al system: An all-in-one solid-phase Fenton reagent for generation of hydroxyl radicals under oxalic conditions. *Sci. Total Environ.* 673, 480–488. <https://doi.org/10.1016/j.scitotenv.2019.04.116>. PMID: 30991337.
- Mahinroosta, M., Allahverdi, A., 2018. Hazardous aluminum dross characterization and recycling strategies: A critical review. *J. Environ. Manage.* 223, 452–468.
- Rostami, M., Hassani Joshaghani, A., Mazaheri, H., Shokri, A., 2021. Photo-degradation of P-nitro toluene using modified bentonite based nano-TiO₂ photocatalyst in aqueous solution. *Int. J. Eng.* 34 (4), 756–762. <https://doi.org/10.5829/ije.2021.34.04a.01>.
- Rubio-Clemente, A., Chica, E., Peñuela, G.A., 2015. Petrochemical wastewater treatment by photo-Fenton process. *Water Air Soil Pollut.* 226, 1–18.
- Saber, A., Hasheminejad, H., Taebi, A., Ghaffari, G., 2014. Optimization of Fenton-based treatment of petroleum refinery wastewater with scrap iron using response surface methodology. *Appl. Water Sci.* 4, 283–290.
- Shokri, A., Mahanpoor, K., 2018. Using UV/ZnO process for degradation of Acid red 283 in synthetic wastewater. *Bul. Chem. Commun.* 50 (1), 27–32.
- Srimoke, W., Kanokkantapong, V., Supakata, N., Limmun, W., 2022. Optimising zero-valent iron from industrial waste using a modified air-Fenton system to treat cutting oil wastewater using response surface methodology. *Arab. J. Chem.* 15 (11), 104213.
- Wang, J., Tang, J., 2021. Fe-based Fenton-like catalysts for water treatment: Catalytic mechanisms and applications. *J. Mol. Liq.* 332, 115755.
- Xiong, Z., Lai, B., Yang, P., Zhou, Y., Wang, J., Fang, S., 2015. Comparative study on the reactivity of Fe/Cu bimetallic particles and zero valent iron (ZVI) under different conditions of N₂ air or without aeration. *J. Hazard. Mater.* 297, 261–268.
- Yuan, Y., Lai, B., Yang, P., Zhou, Y., 2016. Treatment of ammonium wastewater by the combined Fe⁰/air and Fenton process (1stFe⁰/air-Fenton-2ndFe⁰/air). *J. Taiwan Inst. Chem. Eng.* 65, 286–294.
- Zhang, Y., Liu, C., Xu, B., Qi, F., Chu, W., 2016. Degradation of benzotriazole by a novel Fenton-like reaction with mesoporous Cu/MnO₂: combination of adsorption and catalysis oxidation. *Appl. Catal. B* 199, 447–457.